# A potential model for the study of ices and amorphous water: TIP4P/Ice

J. L. F. Abascal, E. Sanz, R. García Fernández, and C. Vega

*Departamento de Química Física, Facultad de Ciencias Químicas, Universidad Complutense,*
*28040 Madrid, Spain*

The ability of several water models to predict the properties of ices is discussed. The emphasis is put on the results for the densities and the coexistence curves between the different ice forms. It is concluded that none of the most commonly used rigid models is satisfactory. A new model specifically designed to cope with solid-phase properties is proposed. The parameters have been obtained by fitting the equation of state and selected points of the melting lines and of the coexistence lines involving different ice forms. The phase diagram is then calculated for the new potential. The predicted melting temperature of hexagonal ice (Ih) at 1 bar is 272.2 K. This excellent value does not imply a deterioration of the rest of the properties. In fact, the predictions for both the densities and the coexistence curves are better than for TIP4P, which previously yielded the best estimations of the ice properties. © *2005 American Institute of Physics.*
[DOI: 10.1063/1.1931662]

## I. INTRODUCTION

In addition to the importance of water in our everyday life, the study of water is of great interest because of its unusual properties. Besides, this "anomalous" behavior[1] is shown by a molecule with an extremely simple chemical formula. Thus, the study of the properties of water is not only of highly practical and technical interest, but also a fundamental scientific challenge. One of the most intriguing properties of water is its rich phase diagram. There are 13 known solid polymorphs—nine of which are stable over a certain range of temperature and pressure—with varying degrees of orientational disorder.[2,3] Although hexagonal ice Ih is the only solid water form found on the earth, medium-pressure and even high-pressure forms of ice probably occur on the solar system.[4] Somewhat surprisingly, it has been argued that most of the water present in the universe is in amorphous form.[5] Moreover, it is widely accepted that liquid water's unusual behavior is a remnant of the more pronounced low-temperature anomalies.[6] Despite the interest in the crystalline and amorphous water forms, most of the work done on this region of the phase diagram of water is experimental. There is a lack of theoretical and/or simulation studies that could help explain the rich behavior of solid water phases.

In the past, water models have been necessarily parametrized in restricted conditions (for an appraisal of the results for different models see, for instance, the review by Guillot[7]). Former water potentials were fitted for single-temperature quantities.[8–10] Besides, the limited computing available power forced to reduce the range of the Coulomb interactions. The molecular geometry was constrained to a set of three or four interaction sites with constant angles and bond lengths. A final simplification was the use of pair potentials, thus neglecting important polarization terms (although these contributions are incorporated to some extent in an effective way). In spite of their limitations, these simple models lead to quite acceptable predictions for the thermodynamic properties of liquid water. After this initial impulse in the early 1980s, there were numerous attempts to overcome the simplicity of the former potential models. Most of the efforts were concentrated on the explicit inclusion of the polarizability, but there have also been attempts to introduce the flexibility of the molecule by allowing intramolecular vibrations. Unfortunately, except perhaps some quantities which cannot be accounted for by simple models due to the intrinsic nature of the potential, the effort in using polarizable models had little advantage over simple models, especially if the increased computing cost is considered. In this way, at the beginning of the new millennium, the majority of the computer simulation work on water is still based on the rigid water models proposed in the 1980s.

In recent years there has been a new surge of water potential models.[11–18] A significant part of this work corresponds to an update of old models. There are several reasons for this. First, it is now possible to make a fit for a wide range of properties and states.[12,14,17] On the other hand, it is well known that the truncation of the electrostatic terms results in changes in the water properties. In particular, significant discrepancies have been reported between the densities calculated with and without truncated long-range forces. The use of a cutoff radius leads to higher densities and shifts the temperature of maximum density at 1 bar to lower temperatures.[17,19,20] Hence, a number of new potentials are a variant of a well-known rigid model, but adapted to their use with a proper treatment of long-range forces.[11,17,21] Finally, the increasing computational power allows one to increase the number of interaction sites of the water molecule, and some new models explore this way.[12,16] Of particular interest are the TIP5P,[12,19,21] TIP4P/Ew,[17] and the six-site model of Nada and van der Eerden.[16] TIP5P is a rigid five-site model designed to reproduce the liquid densities at different temperatures and 1 atm pressure. Besides, the reported values for the TIP5P ice Ih melting temperature at 1 bar are close to

**122**, 234511-1

the experimental result.[16,22,23] TIP4P/Ew (Ref. 17) is a reparametrization of TIP4P for use with Ewald sums and has proven to account for a number of quantities of liquid water, including an excellent prediction of the temperature of maximum density. Although the model proposed by Nada and van der Eerden gives excellent predictions for the melting properties, its computational cost is more than double that of TIP4P. Because of this, and before proceeding with costly computations, it is important to know whether or not a less demanding model is able to account for the properties of the different solid water forms.

The aim of this paper is to check whether or not any of these rigid water models gives acceptable predictions of the ice's properties. We focus our attention on the equation of state of the various ice forms and on the phase equilibria involving at least one crystalline phase. It is concluded that none of the models account satisfactorily for the ice's properties. We then propose a new model and calculate its properties. Section II describes the technical aspects of the simulations. In Sec. III we discuss the predictive ability of the most currently used water models. Then, the procedure for the determination of a new potential is presented. Section IV gives the results for the equation of state and the phase diagram using the new ice model. A final section discusses the main conclusions of this work.

## II. THE SIMULATIONS

Common rigid models place a Lennard-Jones (LJ) interaction site at the oxygen and electrostatic charges at different points of the molecule. In our simulations, the LJ potential was truncated for all phases at 8.5 Å. Standard long-range corrections to the LJ energy were added. The Ewald summation technique has been employed for the calculation of the long-range electrostatic forces. The screening parameter and the number of vectors in the reciprocal space considered had to be carefully selected for each crystal phase. The number of molecules for the different phases was chosen so as to fit at least twice the cutoff distance in each direction. The simulations have been carried out at constant pressure and temperature (NpT). Isotropic NpT simulations are adequate for the liquid phase, while anisotropic Monte Carlo simulations (Parrinello–Rahman-type)[24,25] are required for the solid phases.

Initial configurations were prepared as follows. For the disordered phases (Ih, Ic, IV, VI, and XII) we used the algorithm of Buch *et al.*[26] to generate a starting configuration having no net dipole moment and where the hydrogens (but not the oxygens) are disordered and satisfy the ice rules.[27,28] For the proton ordered phases [ice II, IX, and the antiferroelectric analogous of ice XI (Ref. 29)] we used crystallographic information to generate an initial solid configuration. Notice that, since we are using Parrinello–Rahman NpT, the solid phase is able to change the shape of the simulation box, and therefore that of the unit cell. Ices III and V are known to exhibit only partial disorder.[30] We generalized[31] the algorithm given in Ref. 26 in order to generate an initial configuration with a biased occupation of the hydrogen positions.

For the calculation of the phase diagram we have fol-

lowed the method of Kofke,[32,33] usually denoted as Gibbs–Duhem integration. It consists of the integration of the Clapeyron equation. The classical Clapeyron equation reads

$$\frac{dp}{dT} = \frac{\Delta h}{T \Delta v}. \tag{1}$$

This first-order differential equation (or its inverse $dT/dp$) has been integrated using a fourth-order Runge–Kutta algorithm. The integration requires the computation of the enthalpy and the volume of the two coexisting phases. We have taken advantage of the intrinsic parallelism of the problem to assign the calculation of the enthalpy of each of the phases to one of the CPUs of a dual processor node. The calculation of the liquid water enthalpies is somewhat more demanding and requires comparatively longer simulation runs. Typically, 22 000 cycles were used for determining the enthalpies of the liquid (a cycle is defined as a trial move per particle plus a trial volume change). For the properties of the ice forms, we used the number of cycles that approximately balanced the computational cost of the liquid phase. The integration of the Clapeyron equation requires an initial coexistence point. The initial points may be obtained from free-energy calculations (see Ref. 34 for details). This was the procedure for the TIP4P and SPC/E models. Recently, it has been demonstrated that the starting points of a given model may be accurately obtained from those of a different potential using a generalized Clapeyron equation. A complete description of the method can be found in Ref. 23. For completeness we sketch here a brief summary of this "Hamiltonian" Gibbs–Duhem integration. Let us write a given pair potential in terms of a reference potential as a function of parameter $\lambda$

$$u = (1 - \lambda) u_{\mathrm{ref}} + \lambda u_{\mathrm{new}}. \tag{2}$$

When $\lambda = 0$, $u = u_{\mathrm{ref}}$ and for $\lambda = 1$, it follows that $u = u_{\mathrm{new}}$. We can use $\lambda$ as a new intensive thermodynamic variable so that a change in Gibbs free energy per particle is given by

$$dg = - s dT + v dp + x_g d\lambda. \tag{3}$$

It can be shown that the conjugate thermodynamic variable $x_g$ is

$$x_g = \frac{1}{N} \left\langle \frac{\partial U(\lambda)}{\partial \lambda} \right\rangle_{N,p,T,\lambda}. \tag{4}$$

From this result, following the same steps leading to the classical Clapeyron equation, it is easy to write the generalized relationships

$$\frac{dT}{d\lambda} = \frac{\Delta x_g}{\Delta s} \tag{5}$$

and

$$\frac{dp}{d\lambda} = - \frac{\Delta x_g}{\Delta v}. \tag{6}$$

These equations make possible the calculation of the shift in the coexistence temperature (or pressure) produced by a change in the interaction potential at constant pressure (or temperature). We have checked that the Hamiltonian Gibbs–Duhem integration results are in very good agreement with

TABLE I. Densities (in g cm$^{-3}$) of several ice forms at the temperatures and pressures indicated. The last two rows are the mean value of the (signed) deviations from the experimental data $\bar{d}=\Sigma d/N$ ($d=\rho-\rho_{exp}$) and $\sigma_N = \sqrt{\Sigma d^2/N}$. The SPC/E and TIP4P results come from Ref. 34. The experimental data are taken from Ref. 2.

| Ice | $T$ (K) | $p$ (MPa) | TIP5P | SPC/E | TIP4P | TIP4P/Ew | TIP4P/Ice | Expt. |
|---|---|---|---|---|---|---|---|---|
| Ih | 250 | 0 | 0.976 | 0.944 | 0.937 | 0.935 | 0.909 | 0.920 |
| Ic | 78 | 0 | 1.026 | 0.971 | 0.964 | 0.960 | 0.929 | 0.931 |
| II | 123 | 0 | 1.284 | 1.245 | 1.220 | 1.219 | 1.183 | 1.170 |
| III | 250 | 280 | 1.185 | 1.171 | 1.175 | 1.168 | 1.147 | 1.165 |
| IV | 110 | 0 | 1.371 | 1.324 | 1.314 | 1.308 | 1.276 | 1.272 |
| V | 223 | 530 | 1.331 | 1.294 | 1.294 | 1.289 | 1.255 | 1.283 |
| VI | 225 | 1100 | 1.447 | 1.403 | 1.406 | 1.399 | 1.360 | 1.373 |
| IX | 165 | 280 | 1.231 | 1.219 | 1.210 | 1.202 | 1.174 | 1.194 |
| XI | 5 | 0 | 1.046 | 0.985 | 0.976 | 0.970 | 0.938 | 0.934 |
| XII | 260 | 500 | 1.340 | 1.313 | 1.314 | 1.312 | 1.282 | 1.292 |
| $\bar{d}$ | | | 0.070 | 0.029 | 0.028 | 0.023 | −0.009 | |
| $\sigma_N$ | | | 0.077 | 0.038 | 0.031 | 0.027 | 0.014 | |

the free-energy calculations for the TIP4P and SPC/E models.[23] We have also shown that consistent results for the liquid-ice Ih coexistence temperature of TIP5P are obtained irrespective of the starting potential $u_{ref}$ (TIP4P and SPC/E). Eight λ values were needed to go from SPC/E to TIP4P. The models investigated in this work are relatively similar to TIP4P, so that an integration using only three λ points has proven to be accurate enough for the transit from the TIP4P coexistence properties of one model to the desired model. In the Runge–Kutta algorithm, four different evaluations are required to go from a value of λ to the next one. Thus, about 90 000 cycles were performed for each λ value.

## III. MODEL POTENTIAL FOR SOLID WATER

### A. Ice's properties for commonly used rigid models

In contrast with the great number of computer simulation work done on liquid water properties, the investigation of the physico-chemical quantities of ice forms is rather limited.[18,35–39] The fluid–solid equilibria have been considered by a relatively small number of researchers such as Gao *et al.*[40] van der Eerden and co-workers,[16,41] Clancy and co-workers,[42,43] Haymet and co-workers,[20,44] Woo and Monson,[45] and ourselves.[23,34,39,46] Another source of computer simulation studies of the solid state of water is the investigation of amorphous phases (see the review by Debenedetti[6] on supercooled and glassy water). Although these studies have often been centered around the possible existence of a liquid–liquid transition line ending at a second critical point,[47,48] there is a renewed interest on the study of crystalline–amorphous transitions.[49,50]

The vast majority of the studies rely on the use of simple rigid and nonpolarizable models of water. Gay *et al.* have reported[51] a molecular-dynamics study of the melting and stability of ice Ih using the SPC/E model of water. The calculated density of ice Ih at 250 K differs from the experimental one by 2.5%. Using Monte Carlo simulation, we have obtained an almost identical result for the same system.[34] Ayala and Tchijov[37] have computed the specific volumes of ices III and V in a molecular-dynamics study using the

TIP4P and TIP5P water models. The calculated values for TIP4P are in good agreement with the measured values: the maximum relative error for both III and V forms is less than 1.2%. The deviation of the predictions for the TIP5P model are much larger: over 2% for ice III and around 4% for ice V. Again, our results for these systems using the TIP4P potential[34] are coincident with the findings of Ayala and Tchijov. There is also a recent report[18] of the ice Ih densities close to 0 K using the SPC, SPC/E, TIP4P, and TIP5P models. All the models predict too high densities, especially TIP5P for which the computed value differs by 7% from experiment.

Table I shows our results for the densities of most of the known ice forms. These calculations indicate that all the models overestimate the ice's densities, although in different degrees. TIP5P yields too high densities, the maximum relative deviation from experiment reaching 12% for ice XI. The TIP4P model accounts more or less satisfactorily for the densities of ices Ih, III, V, VI, IX, and XII (the deviation from the experimental values are lower than 3% in all cases). The agreement is less satisfactory for ices II, IV, and XI. The densities for the TIP4P/Ew model are very similar to those for TIP4P. The results for the SPC/E model are also close to those for TIP4P, the only exception being ice II, which is too high in SPC/E. In summary, with the exception of TIP5P which yields too high densities, the equation of state of the various ice forms are relatively well predicted with rigid nonpolarizable models. More importantly, the equation of state of several ice forms does not discriminate the relative merits of TIP4P, TIP4P/Ew, and SPC/E models.

The investigation of the phase diagram of water has revealed it as a stringent test for water potentials. In a recent study, we have shown that the TIP4P model provides a qualitatively correct description of the phase diagram.[34] Ices Ih, II, III, V, VI, VII, and VIII were found to be stable phases for the TIP4P model (as they indeed are for real water). Also in accordance with experiment, ice IV and ice IX are clearly metastable phases for TIP4P. In contrast with the predictions for TIP4P, the SPC/E phase diagram was not satisfactory. A major defect of the SPC/E model is that it predicts that ices

III and V are metastable, which is in clear disagreement with experiment. It also yields a I–II–liquid triple point at $T=215.2$ K and $p=-60$ bar: the stable phase at $p=1$ bar for the SPC/E model is not ice Ih, but ice II. In summary, although both models show similar performance when describing liquid water and ice densities, it is clear that such similarity breaks down when the global phase diagram is considered. TIP5P results are striking. Although this model provides an excellent estimate (274 K) of the melting temperature of hexagonal ice, it has been shown that (as for SPC models) ice II is more stable than ice Ih at ambient conditions.[23]

A study specifically devoted to the melting of ice Ih at $p=1$ bar also gives important information on the predictive ability of different water models.[23] The melting temperatures of ice Ih for SPC, SPC/E, and TIP4P models at $p=1$ bar are $T=190$, 215, and 232 K, respectively.[23] This is at least 40° below the experimental value. Slightly better is the melting temperature yielded by TIP4P/Ew, 245 K. As commented above TIP5P matches the experimental melting temperature. Nevertheless, the coexistence densities are not described satisfactorily by this model. More importantly, the difference between the liquid and solid densities $\rho_l-\rho_{Ih}$ is far too low, 0.015 g/cm³, to be compared with the experimental result, 0.082 g/cm³. As a consequence, the slope of the coexistence line $dp/dT$ at the melting point is five times larger than the experimental one.[23] Models which have demonstrated their usefulness in predicting liquid-phase properties are not completely satisfactory for the study of the melting of ice Ih. Moreover, SPC, SPC/E, and TIP5P do not predict the stability of ice Ih at ambient conditions. According to the predictions for these models, ice II would be a more stable form.[23,34] TIP4P yields quite acceptable densities of several ice forms, but the agreement with the experimental phase diagram is only qualitative, the melting temperature of ice Ih being 40° lower than the experimental one. Similar comments apply to TIP4P/Ew (the rest of the phase diagram is still unknown for this model). It seems clear that there is room for improvement. In the next paragraphs we discuss the parametrization for a model intended for a better description of the solid phases of water.

## B. A two-step parametrization

Our aim is to construct a rigid model which could be useful to represent the properties of solid phases. It has been commented in the previous section that the TIP4P model yields reasonable ice properties. Thus we have selected for our model the TIP4P geometry (which is just the Bernal–Fowler geometry) and functionality. There are four interaction sites. Three of them are placed at the oxygen and hydrogen atom positions, respectively. The other site, often called the $M$ site, is coplanar with the O and H sites and is located at the bisector of the H-O-H angle. As in the original Bernal–Fowler and TIP4P models, we have fixed the O-H distance and H-O-H angle to the experimental values, 0.9572 Å and 104.52°. The total potential energy of the system is the sum of the pair interactions between molecules. The intermolecular pair potential has two contributions, a Lennard-Jones $u_{LJ}$

term and an electrostatic interaction $u_{electrostatic}$. An important feature of the model is that the oxygen site carries no charge, but contributes to the LJ term. The expression for the LJ interaction between two molecules is

$$u_{LJ} = 4\epsilon[(\sigma/r_{OO})^{12} - (\sigma/r_{OO})^6], \tag{7}$$

where $r_{OO}$ is the distance between the oxygen sites of two molecules. Conversely, the H and $M$ sites are charged, but do not contribute to the LJ term. The electrostatic potential between molecules $i$ and $j$ is then

$$u_{electrostatic} = \frac{e^2}{4\pi\epsilon_0}\sum_{a,b}\frac{q_a q_b}{r_{ab}}, \tag{8}$$

where $e$ is the proton charge, $\epsilon_0$ is the permittivity of vacuum, and $a$ and $b$ stands for the charged sites of molecules $i$ and $j$, respectively. As a consequence of the molecular geometry and potential definitions, there are four unknown parameters to determine, namely, the strength $\epsilon$ and size $\sigma$ of the LJ center, the hydrogen site charge (or the charge of the $M$ site, $q_H=-q_M/2$), and the distance $d_{OM}$ between the oxygen and the $M$ site.

The general procedure consists of a first-order expansion of the quantities as a function of the parameters. Thus, for a given property $\psi$ we may write

$$\psi \simeq \psi_0 + \sum_{i=1,4}\frac{\partial\psi}{\partial\xi_i}(\xi_i - \xi_i^0), \tag{9}$$

where $\xi_i$ denotes a parameter in the set $\xi=\{\epsilon,\sigma,q_H,d_{OM}\}$. The procedure requires the knowledge of a selected set of quantities for a starting model potential $\psi_0=\psi(\xi^0)$ and the derivatives with respect to the parameters. In this way, the determination of the four model parameters is done by a nonlinear fit of the selected set of $m$ properties that minimizes the square of the weighted deviations with respect to the experimental values

$$\sum_{j=1,m} w_j(\psi_j - \psi_j^{expt})^2 = \text{min.} \tag{10}$$

The derivatives can be computed numerically. A simple and trivial recipe uses the computed values of the quantity at two values of the parameter (symmetrically placed with respect to the starting parameter), while fixing the rest of the variables. Notice that, in this method, the properties at the starting potential are not used for the calculation of the derivatives, which is a waste of available information. On the other hand, the dependence of a quantity on the parameters is not necessarily linear. Thus, such parametrization procedure would be only approximate, and the final properties would differ from those predicted in the fit. Thus, we decided to simplify the calculation of the derivatives and to undertake the parametrization in two steps. For the calculation of the derivatives, we used only one point additional to that at which the property is initially known,

$$\frac{\partial\psi}{\partial\xi_i} = \frac{\psi(\xi_i,\xi_{\nu\neq i}^0) - \psi(\xi^0)}{\xi_i - \xi_i^0}. \tag{11}$$

The calculated derivatives are somewhat less accurate than that obtained with the symmetric differentiation. But, in the

second parametrization step, the intermediate potential is close enough to the final result, so that both the linear approximation and the algorithm for computing the derivatives introduce negligible errors in the predicted quantities. The final computing cost is about the same as that of a one-step parametrization using symmetric point derivatives (not using the initial state), but the overall procedure is more reliable. Notice finally that the purpose of the fit is the calculation of the parameters. Thus, Eq. (9) is only used in the fitting procedure. Once the model parameters are known, the final properties of the new potential are obtained in Hamiltonian Gibbs–Duhem simulation starting at TIP4P. In other words, there are no approximations for the properties of the final model (apart from those intrinsic to the simulation procedure).

## C. The TIP4P/Ice potential

The densities of the various ice forms are obvious candidates for the fitting procedure. Besides, we have recently shown that it is feasible to calculate a coexistence point for a given model from that for a different model using a generalized Gibbs–Duhem integration.[23] Then it makes sense to include in the fit coexistence points involving different ice forms and liquid water. This is very important as it has been shown that the phase diagram is a stringent test of water-model potentials.[34] In particular, we have observed that several models fail because they predict a too stable ice II form. For this reason we have not fitted any coexistence points involving ices II and III; instead, we have fitted the range of existence of ice III estimated as the difference between the coexistence temperatures of lines II–III and III–liquid at 3 kbar. This usually ensures that ice Ih is the most stable form at ambient conditions. The set of properties used in the first step of the parametrization procedure consists in the melting temperature of ice Ih at 1 bar, the range of existence of ice III at 3 kbar, the densities of three different water phases (liquid water at 300 K, 1 bar; ice II at 123 K, 1 bar; and ice V at 223 K, 5300 bar), and the enthalpy of vaporization at 300 K. The reasons for this particular choice are explained in the following paragraphs.

The heterogeneity of the input data forced us to introduce weighting factors in the fitting procedure. The relative weights are rather arbitrary. The initial guidance can be to assign them more or less inversely proportional to the magnitude of the quantities involved (e.g., as melting points are of the order of 250 K and densities are about 1 g/cm$^{-3}$, the ratio of the corresponding weights may be around 1/250). Despite that, there is still a considerable freedom for the choices of the weight factors, especially because some properties are more important than others. For instance, it seems reasonable to give more importance to the melting temperature of hexagonal ice than to the density of ice V. In summary, even if the derivatives are known for the selected set of properties, the search for a new potential is not automatic.

We have analyzed the dependence of the properties on the potential parameters to simplify the problem of finding the best parameters. From this analysis several important consequences emerge. First of all, it is clear that there is no

possibility to bring the coexistence pressure of ice VII close to experiment. The derivatives, with respect to any of the parameters, are too low to significantly move the results towards the experimental data with reasonable values of the potential parameters. This means that the TIP4P interaction type [i.e., a nonpolarizable and rigid four-site model interacting via Eqs. (7) and (8)] cannot serve as a model to describe the properties of ice at extremely high pressures. Besides, although a wide variety of parameters can be obtained by modifying the weight factors, none of them fit satisfactorily the overall quantities. In particular, *it is impossible to simultaneously fit the melting temperature of ice Ih and the enthalpy of vaporization*. In fact, the same applies to the melting curves of the other ices. The choice of a pair potential with a rigid geometry implies that the effect of the electrical polarization should be included in an averaged way. Thus, effective water potentials exhibit larger dipole moments than that of the isolated molecule. There is a growing acceptation of the idea that a self-energy correction[10] should also be included if a comparison is made between the properties of the liquid state and the gas phase.[7] In fact, much of the reparametrization done when using Ewald sums[17] is a consequence of the acceptation of this argument. The correction depends on the difference between the dipole moment of the model $\mu_l$ and that of the gas phase $\mu_g$ and may be approximated by

$$\Delta E_{\text{pol}} = (\mu_l - \mu_g)^2/2\alpha. \qquad (12)$$

In this work we have also included the correction in the calculation of the enthalpy of vaporization.

Despite the introduction of the self-polarization energy, it was still not possible to obtain a set of parameters (starting at the TIP4P model) producing good predictions for the enthalpy of vaporization and for the melting temperature of hexagonal ice. It is important to stress that this is not a consequence of the fitting procedure. In fact, in the first parametrization step we obtained a compromise model. Their properties were computed as well as their derivatives with respect to the parameters. The model is characterized by the following parameters: $\epsilon/k=100.5$ K, $\sigma=3.155$ Å, $q_H=0.5676$, and $d_{OM}=0.157$ Å. For this model, the melting temperature of ice Ih at $p=1$ bar is 254 K (about 20° lower than the experimental melting point). The departure from experiment of the calculated enthalpy of vaporization is about 0.7 kcal mol$^{-1}$ [after the Eq. (12) correction]. Unfortunately, this intermediate model behaves similarly to TIP4P with respect to the parameter derivatives. In summary, our second conclusion regarding the TIP4P geometry is that (irrespective of the particular parameters of any given model) it is unable to account simultaneously for the melting temperature and the enthalpy of vaporization. As we intend to propose a model for the solid/amorphous phases of water, we decided to give a large value for the weight given to the ice Ih melting temperature and to reject the enthalpy of vaporization from the set of fitting properties. In summary, we essentially fit the density of liquid water and the melting temperature of ice Ih, while forcing ice III to have a (reduced) stability interval. The remaining properties, the densities of ices II and V, are only

TABLE II. Parameters of the potential models.

| Model | $\epsilon/k$ (K) | $\sigma$ (Å) | $q_H$ (e) | $d_{OM}$ (Å) |
|---|---|---|---|---|
| TIP4P | 78.0 | 3.154 | 0.520 | 0.150 |
| TIP4P/Ice | 106.1 | 3.1668 | 0.5897 | 0.1577 |

included (with marginal values of the weighting factors) to avoid the odd behavior of the fitting procedure, and could be substituted by several different quantities.

The values of the optimized parameters for the TIP4P/Ice model are given in Table II. The dipole moment and the components of the quadrupole moment are presented in Table III. The resulting dipole moment of the model is higher than that of TIP4P. Notice that opposite to the behavior of the effective dipole moment (which is larger for the rigid models than for an isolated molecule), the effective quadrupole tensor of all the models is smaller than the experimental one. Nevertheless, the values of the TIP4P/Ice model are already quite close to those of the gas phase.

## IV. RESULTS

The calculated densities for several ice forms using the TIP4P/Ice model have been added to Table I (see Sec. III). The number of cycles is 110 000 for liquid water. As commented above, the number of cycles for the ices is that which approximately balances the computational cost of the liquid phase. TIP4P/Ice provides better estimates than other models. In this case, the predicted densities are, in general, lower than the experimental values (notice that the mean deviation is negative). We have also calculated the density of liquid water at 298.15 K. The result obtained in an 800 000-cycles run, $\rho_l$=0.993 g/cm$^{-1}$, is in excellent agreement with the experimental value, 0.997 g/cm$^{-1}$.

Figure 1 shows the phase diagram of the TIP4P/Ice model. Only the stable phases in real water have been considered for the calculations. The melting temperature of ice Ih at $p$=1 bar is 272.2 K, only 1° below the experimental value. The melting properties of ice Ih at $p$=1 bar are given in Table IV. The good value obtained for the melting temperature could be expected as a consequence of a large value used for the corresponding weight in the fitting procedure. In addition to the excellent agreement of the melting temperature, TIP4P/Ice also provides very accurate results for the volume phase change and for the melting enthalpy. As a consequence, the slope of the $p$-$T$ coexistence line is also in very good agreement with the experiment. Notice that TIP5P also accurately predicts the melting temperature, but it fails

TABLE III. Dipole moment and components of the quadrupole moment.

| Model | $\mu$[a] | $Q_{xx}$[b] | $Q_{yy}$ | $Q_{zz}$ |
|---|---|---|---|---|
| TIP4P | 2.177 | 2.20 | −2.09 | −0.11 |
| TIP4P/Ice | 2.426 | 2.50 | −2.36 | −0.14 |
| Gas (expt.) | 1.85 | 2.63 | −2.50 | −0.13 |

[a]Units are $10^{-18}$ esu cm.
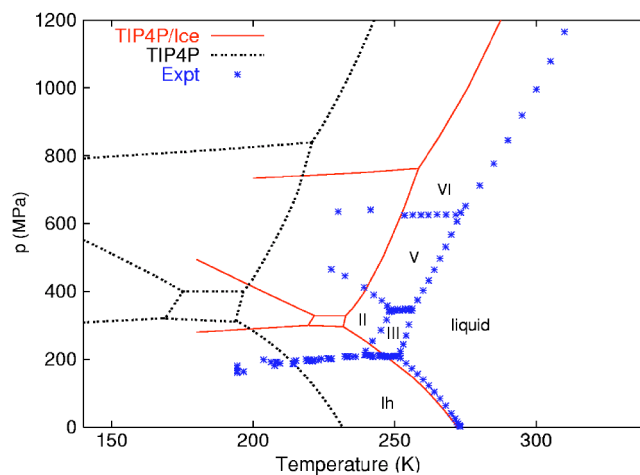[b]Units are $10^{-26}$ esu cm$^2$.



FIG. 1. The phase diagram of TIP4P/Ice (full lines) and TIP4P (dashed) compared to the experiment (stars). The labels mark the domain of stability of the ice phases in the experimental phase diagram.

completely in the prediction of other melting properties, especially the volume change (and the slope of the coexistence line as a consequence).

It is to be noticed in Table IV the large value of the enthalpies for the SPC/E, TIP4P/Ew, and TIP4P/Ice models. This is because these models have built in the self-polarization correction. For this reason we have also presented in Table IV the values of the enthalpies with the correction included. Obviously, the melting enthalpies are not affected by the correction. But, as the correction applies only to condensed phases, the enthalpy of vaporization $\Delta_v H$ *is* affected. The result for TIP4P/Ice at 298 K is $\Delta_v H$ =−11.87 kcal mol$^{-1}$, which is too large compared to the experimental value, −10.52 kcal mol$^{-1}$. It is important to put this result together with the melting enthalpy of ice Ih, $\Delta_m H$. It has already been commented that $\Delta_v H$ has been one important target property in the fitting of most of the water-potential models. Thus, with the exception of TIP4P/Ice, all the models match this property. Table IV shows that the agreement has a cost: the results for $\Delta_m H$ are quite poor for the models with satisfactory $\Delta_v H$. The departures vary from 27% for TIP4P and TIP4P/Ew to 57% for SPC. This seems to be quite a general result since, as with the melting temperatures, our attempts to improve the result for $\Delta_v H$ resulted in worse predictions for the melting enthalpies. The above statement on the impossibility to simultaneously fit the melting temperature of ice Ih and the enthalpy of vaporization is extensive to the melting enthalpy. Notice finally that, in the overall, TIP4P/Ice gives the more balanced results for both enthalpies: the deviations from experiment are 13% for $\Delta_v H$ and 10% for $\Delta_m H$.

All the experimental stable ices appear in the phase diagram of TIP4P/Ice. In fact, the phase diagram has a similar appearance to that of TIP4P, but with better predictions for the coexistence temperatures which are shifted approximately 30−40 K in the direction of the experimental results. The coexistence pressures of ice Ih–ice III, ice III–ice V, and ice V–ice VI are moved towards lower pressures with respect to TIP4P, which also produces a better agreement with the experiment. But despite the improvement, the melting tem-

TABLE IV. Melting properties of ice Ih at $p=1$ bar for different models. $T_m$ is the melting temperature; $\rho_l$ and $\rho_{Ih}$, the densities of liquid water and ice; $H_l$ and $H_{Ih}$, the corresponding enthalpies (the $3RT$ term arising from the translational and rotational kinetics terms is not included); $\Delta_m H$, the melting enthalpy; and $dp/dT$, the slope of the coexistence curve. The rows marked as $H_l^*$ and $H_{Ih}^*$ refer to the enthalpies corrected according to Eq. (12).

| Model | SPC | SPC/E | TIP4P | TIP4P/Ew | TIP5P | TIP4P/Ice | Expt. |
|---|---|---|---|---|---|---|---|
| $T_m$(K) | 190.5 | 215.0 | 232.0 | 245.5 | 273.9 | 272.2 | 273.15 |
| $\rho_l$(g/cm$^3$) | 0.991 | 1.011 | 1.002 | 0.992 | 0.987 | 0.985 | 0.999 |
| $\rho_{Ih}$(g/cm$^3$) | 0.934 | 0.950 | 0.940 | 0.936 | 0.967 | 0.906 | 0.917 |
| $H_l$(kcal/mol) | −11.64 | −12.49 | −10.98 | −12.02 | −10.33 | −13.31 | |
| $H_l^*$ | | −11.24 | | −10.91 | | −11.66 | |
| $H_{Ih}$(kcal/mol) | −12.22 | −13.23 | −12.03 | −13.07 | −12.08 | −14.60 | |
| $H_{Ih}^*$ | | −11.98 | | −11.96 | | −12.95 | |
| $\Delta H_m$(kcal/mol) | 0.62 | 0.74 | 1.05 | 1.05 | 1.75 | 1.29 | 1.44 |
| $dp/dT$(bar/K) | −115 | −126 | −160 | −164 | −708 | −120 | −135 |

peratures of ices III, V, and VI are still about 20–25 K lower than experiment, the difference slightly increasing with pressure. It is not possible to obtain a better fit for these lines, as all the melting curves move as a block for any change in the potential parameters. In this way, the predictions for the melting temperature of ice Ih would deteriorate if the rest of the curves were shifted towards the experimental values. Table V presents the location of the calculated triple points for the TIP4P/Ice model.

Table VI gives the coexistence properties at the triple points. For these computations we have carried out runs similar to those for the integration of the Gibbs–Duhem equation using a processor for each of the two phases in coexistence. With this procedure we get finally two values for each of the phases at a given triple point. The results presented in Table VI use the mean of both calculations. Notice that the interest of a dual calculation is not to duplicate the number of cycles (which could be done in a different way), but to guarantee that the final results are consistent with the first principle of thermodynamics: it is easy to realize that, for the results presented in Table VI, the volume and entropy changes when doing a cyclic transformation are null. Another advantage of the procedure is that it allows a rough estimation of the uncertainty of the phase changes. This is quite different for the transitions involving the liquid state than for those involving only ice phases. Regarding the entropy changes, the uncertainty is probably below 1 J mol$^{-1}$ K$^{-1}$ for the phase changes of liquid water and 0.2 J mol$^{-1}$ K$^{-1}$ for the rest. The situation for the volume changes is a bit more complex as it depends not only on the uncertainty in densities, but also on the magnitude of the change. To give a general idea, the observed differences be-

tween values of the density for the same state are around 3 $\times 10^{-3}$ g/cm$^{-3}$ for liquid water and $3 \times 10^{-4}$ g/cm$^{-3}$ for ices.

In general, the agreement of the results for TIP4P/Ice with experiment is not merely qualitative. For instance the sign of the changes in volume is correct in all cases and the magnitude of $\Delta v$ is quite acceptable: most of them (including those with a low magnitude) present deviations under 20%. Regarding the entropy changes at the triple points, the agreement is also acceptable. For the lines with a large $\Delta S$ (i.e., those involving the liquid state), the departures from experiment are around 20%. The very small value of most of the entropy changes in ice–ice transitions is accurately predicted, but now the relative departures are larger than for the changes in volume. In fact, in a couple of cases, the sign of $\Delta S$ is not correctly predicted. Notice, however, that, in the latter cases, the order of the magnitude of the phase change is comparable to the uncertainty of the computations.

It would be interesting to know if the model gets the correct structure of the liquid. Figure 2 shows the oxygen–oxygen correlation function for TIP4P and TIP4P/Ice. Although the ice model is not intended for the liquid state, it gives a satisfactory description of the liquid water structure. It overestimates the height of the first peak, but gives better predictions than TIP4P for the second coordination shell.

## V. CONCLUDING REMARKS

In this paper we have presented the results for a new potential model (TIP4P/Ice) intended to reproduce the solid phases of water. The new model greatly improves the melting properties of previous potentials (with the possible exception of the Nada and van der Eerden model, which remains to be checked). This is very important in the studies of the equilibrium state, but also out of equilibrium where it is relevant how far the system is from equilibrium. This is the case of nucleation studies or of the investigation of the amorphous phases of water. But, contrary to the case of TIP5P, the improvement in the melting properties is done without deteriorating the other computed quantities. In fact, the TIP4P/Ice model gives also the best overall phase diagram and the best predictions for the densities of several ice forms. It is then useful not only for the investigation of ice Ih, but also for denser ice forms. Finally, a calculation of the density of

TABLE V. Location of several triple points.

| Triple point | $T$ (K) | | $p$ (MPa) | |
| | TIP4P/Ice | Expt. | TIP4P/Ice | Expt. |
|---|---|---|---|---|
| liquid–Ih–III | 231.8 | 251.16 | 295.5 | 209.9 |
| liquid–III–V | 232.6 | 256.16 | 327.0 | 350.1 |
| liquid–V–VI | 258.4 | 273.31 | 763.1 | 632.4 |
| Ih–II–III | 219.4 | 238.5 | 299.0 | 213.0 |
| II–III–V | 221.6 | 248.9 | 328.0 | 344.0 |

TABLE VI. Entropy and molar volume changes at the calculated triple points compared with the corresponding experimental values (taken from Ref. 1).

| | Transition | | $\Delta S$ (J mol$^{-1}$ K$^{-1}$) | | $\Delta v$ (cm$^3$ mol$^{-1}$) | |
|---|---|---|---|---|---|---|
| Triple point | From | To | Expt. | TIP4P/Ice | TIP4P/Ice | Expt. |
| liquid–Ih–III | L | Ih | −14.9 | −16.8 | 3.10 | 2.434 |
| | L | III | −13.9 | −15.3 | −0.59 | −0.839 |
| | Ih | III | 1.0 | 1.6 | −3.69 | −3.273 |
| liquid–III–V | L | III | −13.2 | −18.0 | −0.52 | −0.434 |
| | L | V | −13.1 | −18.3 | −1.53 | −1.419 |
| | III | V | 0.1 | −0.3 | −1.01 | −0.985 |
| liquid–V–VI | L | V | −15.7 | −19.1 | −0.59 | −0.949 |
| | L | VI | −16.2 | −19.2 | −1.35 | −1.649 |
| | V | VI | −0.5 | −0.1 | −0.77 | −0.700 |
| Ih–II–III | Ih | II | −2.1 | −3.2 | −3.97 | −3.919 |
| | Ih | III | 1.0 | 0.7 | −3.71 | −3.532 |
| | II | III | 3.2 | 3.9 | 0.26 | 0.387 |
| II–III–V | II | III | 3.1 | 5.1 | 0.24 | 0.261 |
| | II | V | 3.3 | 4.8 | −0.78 | −0.721 |
| | III | V | 0.1 | −0.3 | −1.02 | −0.982 |

liquid water at 298.15 K and 1 bar indicates that the model could also yield reasonable results for the liquid state.

Obviously, the model has also some limitations. The most evident is the inability to give acceptable predictions of the coexistence lines involving the very dense ice forms VII and VIII. In particular, it predicts that ice VIII is more stable than ice VII. Besides, the triple point liquid–VI–VIII occurs at a pressure of about 6000 MPa, in contrast with the experimental value for liquid–VI–VII which is 2207 MPa. It is important to stress that the situation is similar to that of TIP4P.[34] Notice also that the model behaves quite well for ice VI even at the vicinity of the L–VI–VII triple point. But in the experiment, a denser ice form takes over the phase diagram above 2000 MPa, whereas for TIP4P-type models this form needs a much higher pressure to become a stable phase. The probable reason for this behavior is the limited description of the repulsive forces in both TIP4P and TIP4P/Ice. The model uses only one repulsive site, and this may be a poor representation for ice forms which are only stable when the pressure increases drastically. This means that relatively dense ice forms are satisfactorily described by this model, but it fails for the very dense forms.

The departures of the melting curves of ices III, V, and VI from experiment deserve some comments. More relevant than the magnitude of the deviations is that they are systematic. Although the dependence of the ice's properties on the potential parameters is quite complex, there are clear indications that the excellent prediction for the hexagonal ice melting temperature is related to the high value of the dipole moment. As in the liquid, the description of the interactions in ice requires an effective dipole moment larger than that of the gas phase. Our results suggest that the effective dipole moment is also larger for ice Ih than for the liquid. This fact could explain the departures of the rest of the melting curves, which would be indicative of even larger effective dipole moments in denser ices.
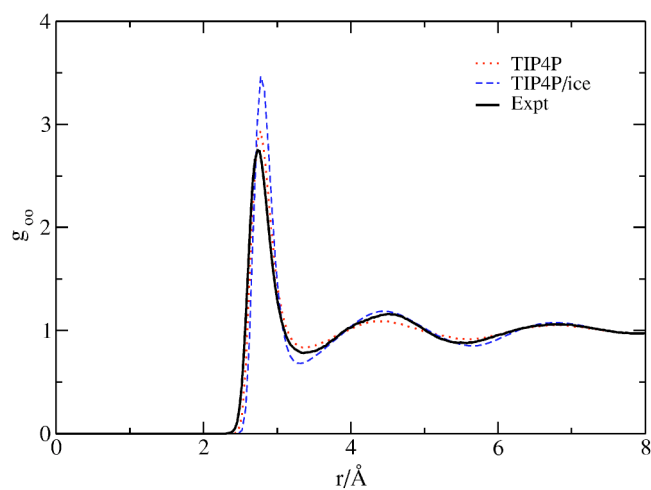
## ACKNOWLEDGMENTS

FIG. 2. Oxygen–oxygen correlation functions at $T=298$ K for TIP4P and TIP4P/Ice models and the experiment (Ref. 52).

[1] D. Eisenberg and W. Kauzmann, *The Structure and Properties of Water* (Oxford University Press, London, 1969).
[2] V. F. Petrenko and R. W. Whitworth, *Physics of Ice* (Oxford University Press, Oxford, 1999).
[3] C. Lobban, J. L. Finney, and W. F. Kuhs, Nature (London) **391**, 268 (1998).
[4] J. P. Poirier, Nature (London) **299**, 683 (1982).
[5] P. Jenniskens and D. Blake, Science **265**, 753 (1994).
[6] P. G. Debenedetti, J. Phys.: Condens. Matter **15**, R1669 (2003).
[7] B. Guillot, J. Mol. Liq. **101**, 219 (2002).
[8] H. J. C. Berendsen, J. P. M. Postma, W. F. van Gunsteren, and J. Hermans, in *Intermolecular Forces*, edited by B. Pullmann (Reidel, Dordrecht, 1981), pp. 333–342.

[9] W. L. Jorgensen, J. Chandrasekhar, J. D. Madura, R. W. Impey, and M. L. Klein, J. Chem. Phys. **79**, 926 (1983).

[10] H. J. C. Berendsen, J. R. Grigera, and T. P. Straatsma, J. Phys. Chem. **91**, 6269 (1987).

[11] D. van der Spoel, P. J. van Maaren, and H. J. C. Berendsen, J. Chem. Phys. **108**, 10220 (1998).

[12] M. W. Mahoney and W. L. Jorgensen, J. Chem. Phys. **112**, 8910 (2000).

[13] C. Burnham and S. Xantheas, J. Chem. Phys. **116**, 1479 (2002).

[14] A. Glättli, X. Daura, and W. van Gunsteren, J. Chem. Phys. **116**, 9811 (2002).

[15] H. Yu, T. Hansson, and W. F. van Gunsteren, J. Chem. Phys. **118**, 221 (2003).

[16] H. Nada and J. P. J. M. van der Eerden, J. Chem. Phys. **118**, 7401 (2003).

[17] H. W. Horn, W. C. Swope, J. W. Pitera, J. D. Madura, T. J. Dick, G. L. Hura, and T. Head-Gordon, J. Chem. Phys. **120**, 9665 (2004).

[18] H. Saint-Martin, B. Hess, and H. J. C. Berendsen, J. Chem. Phys. **120**, 11133 (2004).

[19] M. Lísal, J. Kolafa, and I. Nezbeda, J. Chem. Phys. **117**, 8892 (2002).

[20] T. Bryk and A. D. J. Haymet, Mol. Simul. **30**, 131 (2004).

[21] S. W. Rick, J. Chem. Phys. **120**, 6085 (2004).

[22] Y. Koyama, H. Tanaka, G. Gao, and X. C. Zeng, J. Chem. Phys. **121**, 7926 (2004).

[23] C. Vega, E. Sanz, and J. L. F. Abascal, J. Chem. Phys. **122**, 114507 (2005).

[24] M. Parrinello and A. Rahman, J. Appl. Phys. **52**, 7182 (1981).

[25] S. Yashonath and C. N. R. Rao, Mol. Phys. **54**, 245 (1985).

[26] V. Buch, P. Sandler, and J. Sadlej, J. Phys. Chem. B **102**, 8641 (1998).

[27] J. D. Bernal and R. H. Fowler, J. Chem. Phys. **1**, 515 (1933).

[28] L. Pauling, J. Am. Chem. Soc. **57**, 2680 (1935).

[29] E. R. Davidson and K. Morokuma, J. Chem. Phys. **81**, 3741 (1984).

[30] C. Lobban, J. L. Finney, and W. F. Kuhs, J. Chem. Phys. **112**, 7169 (2000).

[31] L. G. MacDowell, E. Sanz, C. Vega, and J. L. F. Abascal, J. Chem. Phys. **121**, 10145 (2004).

[32] D. A. Kofke, Mol. Phys. **78**, 1331 (1993).

[33] D. A. Kofke, J. Chem. Phys. **98**, 4149 (1993).

[34] E. Sanz, C. Vega, J. L. F. Abascal, and L. G. MacDowell, Phys. Rev. Lett. **92**, 255701 (2004).

[35] M. D. Morse and S. A. Rice, J. Chem. Phys. **76**, 650 (1982).

[36] I. Borzsák and P. Cummings, Chem. Phys. Lett. **300**, 359 (1999).

[37] R. B. Ayala and V. Tchijov, Can. J. Phys. **81**, 11 (2003).

[38] S. W. Rick and A. D. J. Haymet, J. Chem. Phys. **118**, 9291 (2003).

[39] E. Sanz, C. Vega, J. L. F. Abascal, and L. G. MacDowell, J. Chem. Phys. **121**, 1165 (2004).

[40] G. T. Gao, X. C. Zeng, and H. Tanaka, J. Chem. Phys. **112**, 8534 (2000).

[41] M. J. Vlot, J. Huinink, and J. P. van der Eerden, J. Chem. Phys. **110**, 55 (1999).

[42] L. A. Báez and P. Clancy, J. Chem. Phys. **103**, 9744 (1995).

[43] B. W. Arbuckle and P. Clancy, J. Chem. Phys. **116**, 5090 (2002).

[44] T. Bryk and A. D. J. Haymet, J. Chem. Phys. **117**, 10258 (2002).

[45] H.-J. Woo and P. A. Monson, J. Chem. Phys. **118**, 7005 (2003).

[46] C. McBride, E. Sanz, C. Vega, and J. L. F. Abascal, Mol. Phys. **103**, 1 (2005).

[47] P. Poole, F. Sciortino, U. Essmann, and H. E. Stanley, Nature (London) **360**, 324 (1992).

[48] P. H. Poole, F. Sciortino, U. Essmann, and H. E. Stanley, Phys. Rev. E **48**, 3799 (1993).

[49] R. Martoňák, D. Donadio, and M. Parrinello, Phys. Rev. Lett. **92**, 225702 (2004).

[50] C. McBride, C. Vega, E. Sanz, and J. L. F. Abascal, J. Chem. Phys. **121**, 11907 (2004).

[51] S. C. Gay, E. J. Smith, and A. D. J. Haymet, J. Chem. Phys. **116**, 8876 (2002).

[52] A. K. Soper, Chem. Phys. **258**, 121 (2000).